Fibers and Polymers 2014, Vol.15, No.10, 2061-2065 DOI 10.1007/s12221-014-2061-3

Fabrication of Continuous Nanofiber Core-spun Yarn by a Novel Electrospinning Method

Jianxin He[1,2]*, Yuman Zhou[1], Lidan Wang[1], Rangtong Liu[1,2], Kun Qi[1], and Shizhong Cui[1,2]

[1]*College of Textiles, Zhongyuan University of Technology, Zhengzhou 450007, China*
[2]*Henan Key Laboratory of Functional Textile Materials, Zhongyuan University of Technology, Zhengzhou 450007, China*
(Received December 31, 2013; Revised March 26, 2014; Accepted April 18, 2014)

Abstract: Continuously twisted polyacrylonitrile/viscose nanofiber core-spun yarns were fabricated through novel self-designed multi-nozzle air jet electrospinning set-up. The effect of voltage, solution flow rate, air flow rate and funnel rotating speed on coating rate of core-spun yarn, nanofiber diameter, twist level and mechanical property were discussed. The results showed that polyacrylonitrile/viscose nanofiber core-spun yarns with perfect nanofiber orientation and uniform twist distribution could be obtained at voltage of 32 KV, solution flow rate of 32 m*l*/min and air flow rate of 1000 m*l*/min, and the spinning speed could reach to 235.5 cm/min. The diameters of outer coated nanofiber distributed from 100 nm to 300 nm, and nanofiber coating rate could reach to 70.4 %. In addition, the strength and elongation at break increased from 30.82 MPa to 69.65 MPa and from 28.34 % to 43.29 % at the twist angle of 46.6 °, respectively.

Keywords: Multi-nozzle, Air jet electrospinning, Nanofiber core-spun yarns, Coating rate, Mechanical property

Introduction

Traditional core-spun yarn is defined as a kind of yarn with special structure of a continuous filament or staple fiber yarn as core yarn and surrounded by staple fibers outside [1]. Physical properties of core yarn and special characteristics of outer staple fibers can be utilized simultaneously for core-spun yarn [2,3]. Electrospun nanofibers with nanometric diameter, large specific surface area and small pore size have found vast application potential in protective clothing, biomaterials, tissue scaffolds, sensor and filtration [4,5]. However, most of electrospun fibers are produced in the form of randomly oriented non-woven fiber mats. The relatively low mechanical strength and the difficulty in tailoring the fibrous structure have restricted their applications [6,7]. Nanofiber core-spun yarns can be obtained if coating nanofibers on conventional yarn surface. Thereby, nanofiber core-spun yarns not only have the strength of conventional yarn, but also have characteristics of nanofibers. In addition, this yarn can be processed through conventional textile methods to build all kinds of functional structural materials.

At present, nanofibers had been coated on yarn or fabric surface to get functional application [8,9]. Ding [10] reported a new approach for fabricating a super-hydrophobic nanofibrous zinc oxide (ZnO) film surface through a simple electrospinning coating technology. Gogotsi [11] obtained titanium dioxide-coated nanofiber filters by electrospinning polyamide nanofibers onto the surface of a conventional filter followed by electrospraying a suspension of nanocrystalline titanium dioxide onto the electrospinning nanofibers. Scardino [12] created a continuous nanofiber yarn consisting of a core filament yarn with random electrospun fibers on the surface. Dabirian [13] developed a process to produce continuous core-spun yarns from oppositely charged electrospun nanofibers.

However, it is still a huge challenge to prepare nanofiber core-spun yarns with higher yield. Multi-nozzle air jet electrospinning was proposed to fabricate continuous twisted nanofiber core-spun yarns and the effects of voltage, solution flow rate, air flow rate and funnel rotating speed were discussed here.

Experimental

Preparation of Spinning Solution

Polyacrylonitrile (PAN, M_w 60,000) solution of 15 wt% concentration was prepared through dissolving PAN powder in N-N dimethyl formamide (DMF) solution at 80 °C for 3 h.

Preparation of Nanofiber Core-spun Yarn

Multi-nozzle air jet electrospinning set-up used to spinning continuous viscose filament/PAN nanofiber core-spun yarn was shown in Figure 1, including spinning unit, fluid reservoir, metering pump, constant flow air pump, metal funnel, yarn guide roller and winder device. Spinning unit consisted of nozzle, air chamber, air injection tube, and connecting body (Figure 2). Two groups of spinning units, which connected separately with the positive and negative electrodes of the DC power supply, arranged symmetrically on both sides under metal funnel collector. The metal funnel collector was not earthed.

During experiment, the air was firstly transported to the air chamber of each spinning unit simultaneously with uniform rate by air pump. PAN spinning solution was transported to the nozzle of each spinning unit simultaneously with uniform rate by metering pump. Bubbles (hollow Taylor cone) formed on the mouth of nozzle when the air of air chamber squirted upward through air injection tube. The charged bubbles ruptured into multi-jets and then were stretched by

*Corresponding author: hejianxin771117@163.com

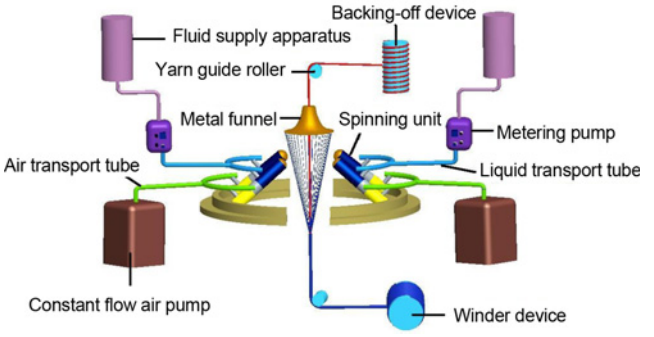

Figure 1. The schematic of multi-nozzle air jet electrospinning set-up.

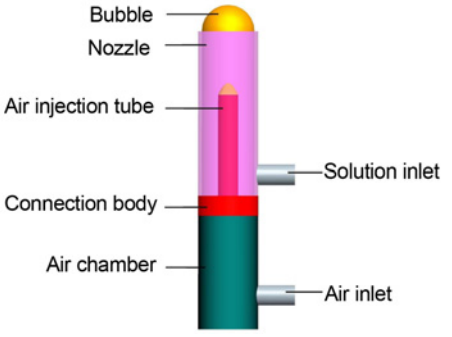

Figure 2. The structure of spinning unit.

the electric force into nanofibers. Core filament yarn passed through metal funnel via yarn guide roller at a constant speed and winded into winder device. An inverted cone-shaped hollow nanofiber web came into being during experiment, one end connected to metal funnel edge and the other connected to corn yarn surface. The nanofiber web was twisted and winded into the surface of traveling core yarn uniformly through the rotation of metal funnel.

Viscose filament yarn (4.6 dtex×60) was used as core filament yarn. A voltage of 30-34 kV was applied to the nozzles with a distance between homopolar nozzles at 7 cm. The distance between positive and negative nozzles was 18 cm. Air flow rate was at a range of 800-1200 m*l*/min. The spinning solution flow rate was varied from 24 to 40 m*l*/h. The funnel collector rotating speed were adjusted in the range of 0-200 r/min. Take-up speed of yarn winder was 30 r/min.

Characterization

The nanofiber yarns collected were coated with gold film in order to observe fiber and yarn morphologies. The instrument was a JEOL JSM-5600LV electron microscopic with an accelerating voltage of 15 kV. The diameters of fiber and yarn and twist angle were calculated based on the SEM images. At least 100 counts were taken for each measurement.

Mechanical Property Measurement

The tensile properties were measured with an INSTRON 5582 tester at room temperature under room humidity. The gauge length was set to be 15 cm and the rate of the crosshead was 150 mm/min. The reported data of breaking strength and elongation represent the average results of 20 tests.

Coating Rate Measurement

The coating rate of nanofiber core-spun yarn was calculated through formula (1). The reported data represent the average results of 20 tests.

$$\text{Coating rate} = \frac{W_1 - W_0}{W_0} \times 100\ \% \quad (1)$$

W_1: the weight of nanofiber core-spun yarn (g),
W_0: the weight of core yarn (g).

Results and Discussion

Spinning Mechanism

The working electric field of multi-nozzle air jet electrospinning was simulated by Maxwell 12.0 (Figure 3). Two pairs of nozzles were positively and negatively charged, respectively, and the funnel collector located in the middle was not earthed [14]. Bubble film formed by polymer solution was stretched, and then burst to generate multiple high-speed jets, and last drawn to nanofibers in the electric field (Figure 4(a)). Furthermore, the conjugate electric field come into being between positive and negative nozzles, and the electric field lines directed from positive nozzles to negative. The uncharged metal funnel located in the middle of two groups of nozzles changed the original distribution of electric field; thereby there have been induction electric fields between the edge of funnel and their nearby charged nozzles. Nanofibers were adsorbed and collected at the edge of funnel and then an inverted cone-shaped hollow nanofiber web was form under the combined action of conjugate electric field and induction electric fields (Figure 4(b)). The web was twisted on core yarn surface through the rotating

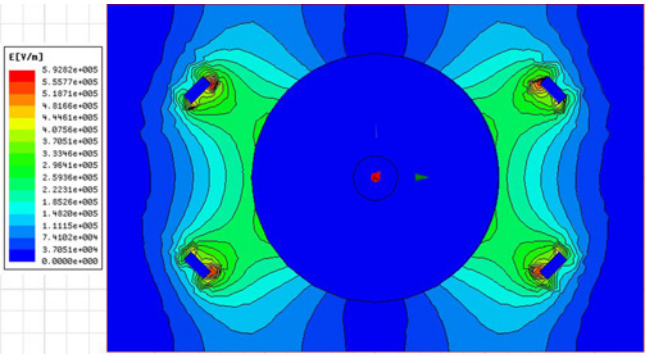

Figure 3. The simulation of multi-nozzle air jet electrospinning working electric field.

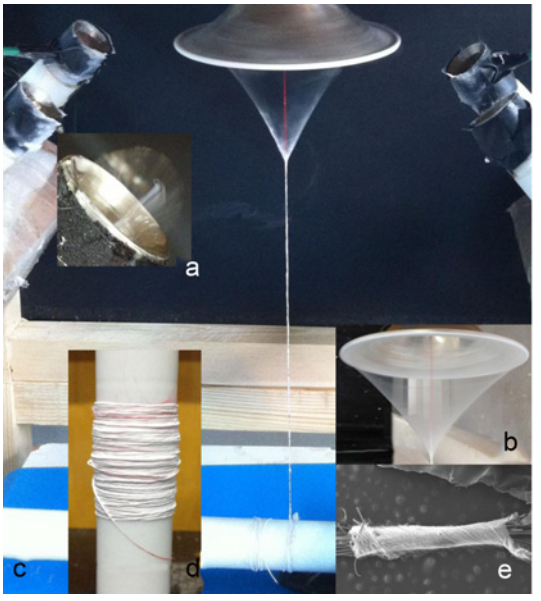

Figure 4. (a) Solution bubble, (b) nanofiber web, (c) the process of preparing nanofiber core-spun yarn, (d) digital camera image of nanofiber core-spun yarn, and (e) the SEM image of nanofiber core-spun yarn.

funnel. Coated nanofibers integrated with core filament yarn well, and nanofiber core-spun yarns fabricated displayed good orientation and uniform twist distribution (Figure 4(c)-(d)). The take-up speed of core-spun yarn could reach to 235.5 cm/min.

Effect of Applied Voltage on Coating Rate of Core-spun Yarn and Nanofiber Diameters

The dependences of core-spun yarn coating rate and nanofiber diameters on applied voltage were shown in Figure 5. Nanofiber diameter decreased with the increase of applied voltage. The decreased nanofiber diameter could be attributed to adequate drafting of jets under a higher voltage. The coating rate of core-spun yarn increased with the increase of applied voltage. When the voltage increased up to 32 kV, the coating rate of core-spun yarn exhibited a maximal value of 70.4 %. The increased coating rate of core-spun yarn can be explained by the increase of fiber scales because bubbles could be drafted adequately and burst to generate more jets at higher voltage. However, the coating rate of core-spun yarn reduced when the voltage exceeded 32 kV. The reason may be that the increase of repulsive force under such a higher voltage between homopolar nozzles led to nanofiber scattering and decreased the aggregation of nanofibers.

Effect of Air Flow Rate on Core-spun Yarn Coating Rate and Nanofiber Diameters

Air flow rate is an important factor affected on the coating

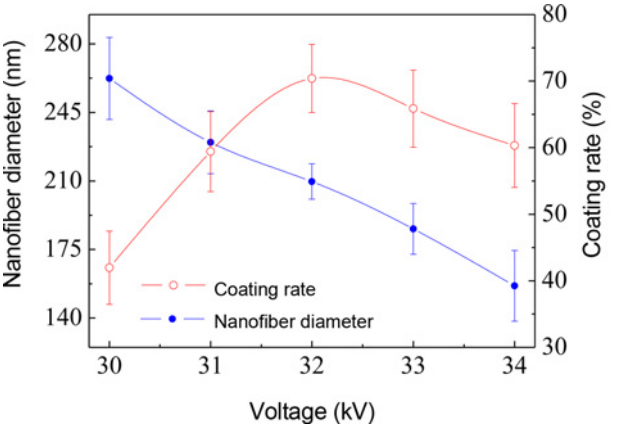

Figure 5. Effect of applied voltage on core-spun yarn coating rate and nanofiber diameters.

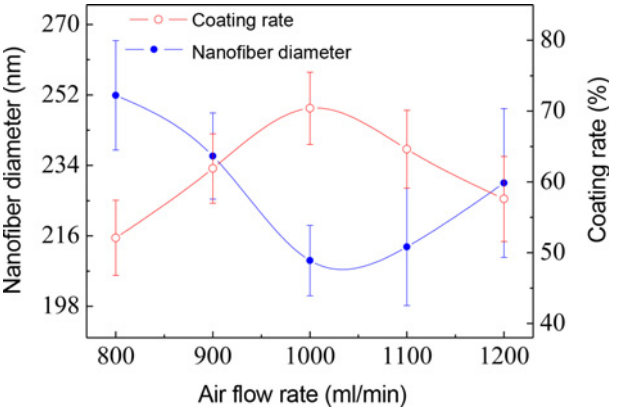

Figure 6. Effect of air flow rate on core-spun yarn coating rate and nanofiber diameters.

rate of core-spun yarn because the improvement of nanofiber production for this air jet electrospinning process was based on the mechanism that bubble could burst to generate multiple jets. Figure 6 showed the dependences of core-spun yarn coating rate and nanofiber diameters on air flow rate. When air flow rate was lower than 800 m*l*/min, core yarn could not be coated completely due to lower nanofiber production. Solution bubbles were difficult to eject from the nozzle and consequently the solution leaked into the chamber under smaller air pressure. The coating rate of core-spun yarn increased notably with the increase of air flow rate, while nanofiber diameter decreased. The coating rate of core-spun yarn exhibited a maximal value of 70.4 % at an air flow rate of 1000 m*l*/min, but nanofiber diameter reached the minimum value. The solution bubbles with large volume and thin wall could form and burst frequently at higher air flow rate when solution flow rate kept stably. Thus nanofiber production increased due to generating more and thinner jets. However, when air flow rate exceeded 1000 m*l*/min, the coating rate of core-spun yarn reduced and nanofiber diameter increased. Solution gushed out directly at such a higher air

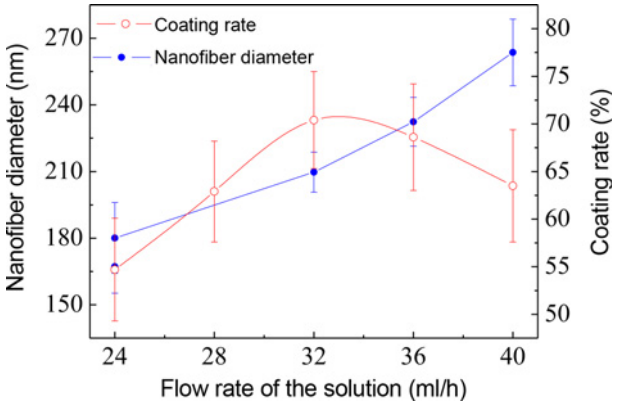

Figure 7. Effect of solution flow rate on core-spun yarn coating rate and nanofiber diameters.

flow rate. Gushing solution almost could not be drafted to nanofibers and interfered with the electric field.

Effect of Solution Flow Rate on Core-spun Yarn Coating Rate and Nanofiber Diameters

Nanofiber diameters increased with the increase of solution flow rate (Figure 7). Solution bubbles with thick wall formed at higher solution flow rate, which burst to fewer thick jets. The coating rate of core-spun yarn increased first with the increase of solution flow rate, and then decreased, when solution flow rate exceed 32 m*l*/h. When solution flow rate was too high, only a portion solution formed bubbles and the rest of solution dropped as droplet from nozzles at such a higher solution flow rate. Overflowed solution interfered with original electric field, and was not stretched to nanofibers by static electricity.

Morphology and Mechanical Property of Nanofiber Core-spun Yarn at Different Funnel Speed

Aggregation and twisting of nanofiber core-spun yarns are relied on unearthed metal funnel, thus the twist level of nanofiber core-spun yarns are dependent on the funnel rotating speed. The SEM images of nanofiber core-spun yarns on different funnel rotating speed were shown in Figure 8. When the funnel rotating speed was less than 150 rpm, nanofibers were coated on the core yarn surface perfectly with a good orientation and a uniform twist distribution, and the twist level of core-spun yarn increased with the increase of funnel rotating speed. Although the twist level of core-spun yarn increased, the more hairiness could be observed on core-spun yarn surface and yarn evenness deteriorated when funnel rotating speed exceed 150 rpm. The morphology of nanofiber core-spun yarn at the cross section was shown in Figure 9. Nanofibers integrated with the core yarn well. However, some micropores could be observed at the interface owing to the irregular shape of the core yarn.

Figure 10 showed the strength and elongation of nanofiber core-spun yarn at break on different funnel rotating speed.

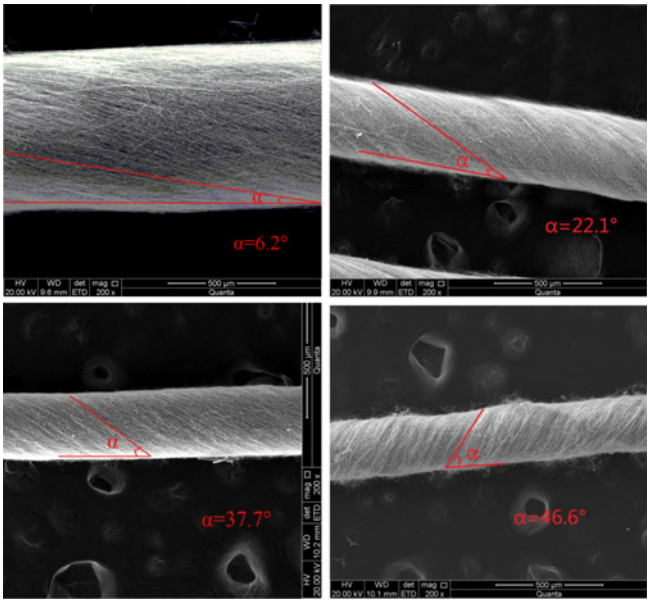

Figure 8. The SEM images of nanofiber core-spun yarns on different funnel speed (200 time).

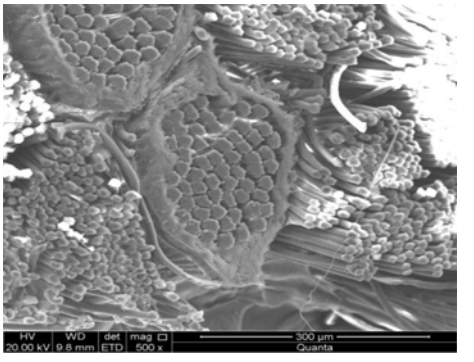

Figure 9. Morphology of nanofiber core-spun yarn at the cross section.

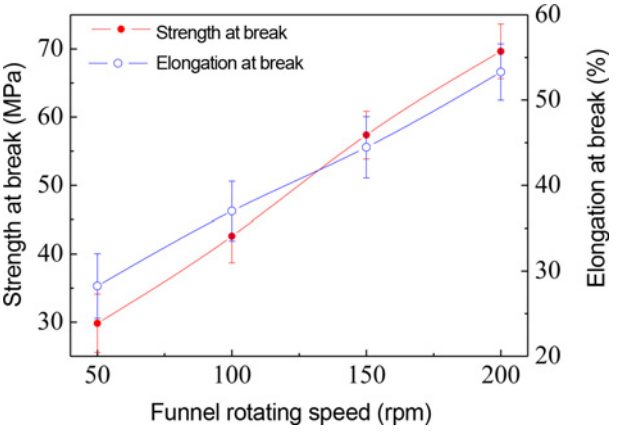

Figure 10. Effect of funnel rotating speed on mechanical property of nanofiber core-spun yarn.

The strength and elongation at break of nanofiber core-spun yarn increased notably with the increase of funnel rotating speed owing to the increase of twist level. The strength and elongation at break increased from 30.82 MPa and 28.34 % to 69.65 MPa and 43.29 %, respectively, when funnel rotating speed increased from 50 rpm to 200 rpm.

Conclusion

Continuously twisted polyacrylonitrile/viscose nanofiber core-spun yarns were prepared by multi-nozzle air jet electrospinning set-up. An amount of nanofibers ejected from spinning units could be twisted on the surface of core filament yarn with good orientation and core-spun yarn take-up speed reached to 235.5 cm/min. The coating rate, winding speed and twist level of core-spun yarn could be adjusted by changing the voltage, solution flow rate, air flow rate and the funnel rotating speed. Twist angle of core-spun yarn could reach to 46.6 ^{o}, and the strength and elongation at break were 69.65 MPa and 43.29 % respectively. Nanofiber core-spun yarns fabricated by this method can be coated one or more kinds of nanofibers and used to prepare functional textiles.

Acknowledgments

This work was supported by a grant from National Natural Science Foundation of China (No. 51203196), and the financial support of the United Foundation from National Natural Science Foundation of China and The People's Government of Henan Province for Cultivating Talents (No. U1204510) is gratefully acknowledged.

References

1. O. Babaarslan, *Text. Res. J*., **71**, 367 (2001).
2. A. P. S. Sawhney, P. Radhakrishnaiah, and T. Sukasem, *Text. Res. J*., **63**, 573 (1993).
3. M. Miao, Y. L. How, and S. Y. Ho, *Text. Res. J*., **66**, 676 (1996).
4. S. Ramakrishna, K. Fujihara, W. E. Teo, T. Yong, Z. Ma, and R. Ramaseshan, *Mater. Today*, **9**, 40 (2006).
5. C. B. Huang, S. L. Chen, C. L. Lai, D. H. Reneker, H. Y. Qiu, Y. Ye, and H. Q. Hou, *Nanotechnology*, **17**, 1558 (2006).
6. W. E. Teo and S. Ramakrishna, *Compos. Sci. Technol.*, **69**, 1804 (2009).
7. W. E. Teo and S. Ramakrishna, *Nanotechnology*, **17**, R89 (2006).
8. F. L. Zhou, R. H. Gong, and I. Porat, *Sur. Coat. Technol*., **204**, 3459 (2010).
9. M. B. Bazbouz and G. K. Stylios, *Eur. Polym. J*., **44**, 1 (2008).
10. B. Ding, T. Ogawa, and J. Kim, *Thin Solid Films*, **516**, 2495 (2008).
11. B. Y. Lee, K. Behler, M. E. Kurtoglu, M. A. Wynosky-Dolfi, R. F. Rest, and Y. Gogotsi*, J. Nano. Res*., **12**, 2511 (2010).
12. F. L. Scardino and R. J. Balonis, *U.S. Patent*, 6308509 (2001).
13. F. Dabirian, S. A. H. Ravandi, J. Hinestroza, and R. A. Abuzade, *Polym. Eng. Sci*., **52**, 1724 (2012).
14. J. X. He, Y. M. Zhou, K. Qi, L. D. Wang, P. P. Li, and S. Z. Cui, *Fiber. Polym.*, **14**, 11 (2013).